Different time regimes of tracer exchange in single-file systems

Sergey Vasenkov and Jörg Kärger*
Fakultät für Physik and Geowissenschaften, Universität Leipzig, Linnéstrasse 5, D-04103 Leipzig, Germany
(Received 13 December 2001; revised manuscript received 26 August 2002; published 19 November 2002)

A complete description of the time dependence of tracer exchange in single-file systems is given. It is based on the combined application of dynamic Monte Carlo simulations and analytical calculations. Depending on the time elapsed, the tracer exchange is found to have different time scaling related to transport modes of either normal diffusion or single-file diffusion. The mode of single-file diffusion is reproduced by recent tracer exchange experiments conducted by laser-polarized ^{129}Xe NMR spectroscopy.

DOI: 10.1103/PhysRevE.66.052601 PACS number(s): 68.43.Jk, 66.30.−h, 68.35.Fx, 82.56.Lz

INTRODUCTION

Stimulated by the advent of zeolites with pore systems consisting of an array of parallel channels of molecular dimensions [1–3], the investigation of single-file diffusion, i.e., of one-dimensional random walk with the exclusion of mutual particle passages, has become a hot topic of fundamental and applied research [4–18]. As a particularly intriguing feature, particle exchange between the interior of the single-file system and its surroundings could not be based anymore on the familiar concept of normal diffusion [19–21]. Therefore, e.g., in the case of catalysis with single-file systems [3,13,15–17], the traditional Thiele concept of correlating transport and reaction [20,21] has to be abandoned. The establishment of a comprehensive theory correlating transport and reaction in single-file systems requires complete knowledge of the kinetics of molecular exchange with the surroundings. So far, in the literature the diffusion in finite single-file systems under equilibrium with the surroundings has been represented in terms of both normal diffusion [9–11] and single-file diffusion [3,18]. In this paper, we report a comprehensive description of the kinetics of molecular exchange, i.e., of the tracer exchange curves, governed by these different diffusion regimes, including all special cases.

SIMULATION RESULTS

Dynamic Monte Carlo (DMC) simulations were performed as described in Refs. [3,9]. At the beginning of a simulation run, the sites of the single-file system are statistically occupied with the probability θ. The particles are allowed to perform jump attempts toward one of the adjacent sites. They are successful if this site is vacant. Jump attempts from the marginal sites are always successful if the jumps are directed outside the system and lead to desorption. Adsorption into the marginal sites occurs at such a rate that the mean occupancy probability θ remains constant. The potential barriers for desorption from the marginal sites in zeolites are usually larger than those for site-to-site hopping. In fact, for sufficiently short single-file systems, tracer exchange may therefore be controlled by the finite exchange rate with the surroundings rather than by intracrystalline diffusion [9–11]. However, the site number of real zeolite channels is typically by orders of magnitude larger than considered in the present simulations so that, for the sake of simplicity, any difference between the potential barriers for desorption and site-to-site hopping may be neglected. The exchange experiment starts by implying that from now on only tagged particles enter the file. As an example, Fig. 1 presents the concentration profiles $q(x,t)$ of tagged molecules at four subsequent times t_i. $\int_{x=0}^{L} q(x,t)dx$ yields the total amount $Q(t)$ of tagged molecules at time t, where the integral stands for the sum over $L=150$, 300, or 600 sites of the single-file system. The ratio $Q(t)/Q(\infty)$ is referred to as the tracer exchange curve $\gamma(t)$. Figure 2 summarizes the results of extensive DMC simulations of tracer exchange in files of length $L=150$, 300, and 600 for the occupation probabilities $\theta=0.25$, 0.50, 0.75, and 0.90. For convenience of presentation, we plotted the product $\gamma(t)L$ rather than the tracer exchange curve $\gamma(t)$ itself. $\gamma(t)L$ denotes the mean number of tagged particles at time t divided by the occupation probability θ. In this way, instead of yielding different curves for any pairs L and θ, the exchange behavior is represented by a much smaller number of master plots. The coincidence of the curves for a given θ for different values of L in Fig. 2 is clearly a consequence of the fact that the time intervals considered are small enough so that there is no correlation be-

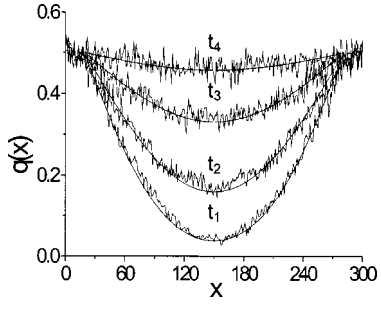

FIG. 1. Comparison of the concentration profiles of tagged particles obtained by MDC simulations for tracer exchange in single-file systems of length $L=300$ (oscillating solid lines) with the concentration profiles for normal diffusion with $D_{(\mathrm{iii})}$ and L^* given in Table I (solid lines) at times: $t_1=0.93\times10^6\times\tau$, $t_2=2.1\times10^6\times\tau$, $t_3=3.7\times10^6\times\tau$, and $t_4=7.6\times10^6\times\tau$ (τ is the duration of the elementary diffusion step).

*Author to whom correspondence should be addressed. FAX: +49 341 97 32549; email address: kaerger@physik.uni-leipzig.de

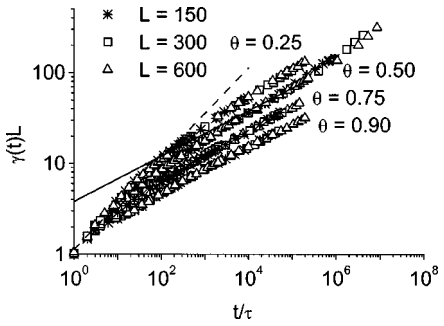

FIG. 2. The normalized tracer exchange curves in single-file systems obtained by DMC simulations for different L and θ (points). The dashed and solid lines show the best fit lines for $\theta=0.5$ with the slopes of $\frac{1}{2}$ and $\frac{1}{4}$ expected for the mechanism of normal and of single-file diffusion, respectively, in the limit of short times.

tween the tracer exchange on the two file margins. This is the situation considered in the time regimes (i) and (ii) in the following analytical treatment.

ANALYTICAL CONSIDERATIONS

The numerical data of Fig. 2 scale with $t^{1/2}$ at short times and approach a $t^{1/4}$ dependence at longer times. In the double-logarithmic representation, these dependences correspond to straight lines with slopes $\frac{1}{2}$ and $\frac{1}{4}$, respectively. We shall refer to them as the time regimes of single-particle diffusion (i) and single-file diffusion (ii). In a third regime, appearing in Fig. 2 only in its initial state for $\theta=0.50$, the center-of-mass diffusion (iii) becomes dominant.

(i) In the regime of single-particle diffusion, $\gamma(t)L$ scales with $t^{1/2}$ for all values of L and θ. It is a consequence of the fact that particle desorption from the marginal sites is not correlated with the movements of the other particles. The spread of particle correlation is limited, therefore, by the distance to the nearest margin, in pronounced contrast to single-file diffusion, where the correlations continuously spread out with time. Thus, it is not unexpected that tracer exchange is initially controlled by single-particle diffusion at the margins. Hence, the short-time approach

$$\gamma_{(\mathrm{i})}(t)=\frac{4}{L}\sqrt{Dt/\pi} \tag{1}$$

of diffusion-limited tracer exchange [22] is in fact found to comply with the initial part of the tracer exchange curve. For each θ, least-squares fits yield diffusivities $D_{(\mathrm{i})}$ in the interval $0.4\times D_0 \leqslant D_{(\mathrm{i})} \leqslant 0.6\times D_0$ (with the free-particle diffusivity $D_0=l^2/2\tau$), independent of L.

(ii) With increasing time the tracer exchange curve is progressively stronger, governed by the transport of more distant particles to the margins. Mutual interactions between the particles experienced on the way to the marginal sites lead to deviations from the mechanism of single-particle diffusion and thus to the onset of a time regime, which is governed by single-file diffusion. In this regime, as in regime (i), the total file length is still much larger than the distance $[\gamma(t)L]$ over which the tagged molecules have penetrated into the single-file system. Hence, their distance distribution remains independent of L. A lower limit for the crossover time between the regimes (i) and (ii) is given by that from mean-field diffusion to single-file diffusion $t_c=1/(\pi D_0\theta^2)$ [10]. The actual crossover time between the regimes (i) and (ii) is found to be larger by a factor less than or equal, 2 which corresponds to the fact that at any time desorption from the marginal sites is not correlated with the movements of the other particles.

We approach this case analytically by assuming that the evolution of the particle arrangement near the margin of a finite single-file system may be modeled by that in an infinitely extended single-file system, the reference system, in which any untagged particle passing a certain point from one (the external) side is converted into a tagged one. The position of the conversion marks the margin of the finite single-file system. Transferring the problem of tracer exchange at the margin of a finite file to molecular propagation in a single file of infinite extension leads to the great advantage that now the propagator is known. As in the case of normal diffusion, the propagator is given by a Gaussian, however with the important difference that the mean square displacement $\langle x^2(t)\rangle$ scales with $t^{1/2}$ rather than with t [23]. This equivalence means in particular that the probability of particle distribution in single-file systems evolves exactly the same way as in the case of normal diffusion, if only the mean square displacement is used as an evolution parameter. Equation (1) may be rewritten, therefore, as

$$\gamma_{(\mathrm{ii})}(t)=\frac{1}{L}\sqrt{8/\pi\langle x^2(t)\rangle} \tag{2}$$

to include simultaneously the cases of normal and single-file diffusion. In the following, we will show that Eq. (2) is in surprisingly good agreement with the exact results derived analytically for single-file diffusion. The procedure is illustrated by Fig. 3. It shows by way of an example, the evolution of the positions of eight adjacent particles in the reference system close to the position $x=0$, which represents the margin of the finite single-file system. The first four columns represent consecutive desorption of particles 5, 4, and 3, which is followed by adsorption of the labeled particles 3 to 7. In contrast to diffusion-limited tracer exchange, the knowledge of the position of the labeled particle with the largest distance from the margin alone is sufficient to determine the number of labeled particles in each particular single-file channel (Fig. 3). This is a consequence of the fact that under the considered boundary conditions no mixture of labeled and unlabeled particles is possible. Hence, the product $\gamma(t)L$ is given by the mean distance between the margins and the tagged molecules with the most remote position from the margin in each channel of the single-file system. In order to calculate this length, we have to determine the probability (density) $P(x_0,x_f,t)$ that a particle, which starts at x_0 and during $0\cdots t$ touches the conversion point $x=0$, finally gets to x_f at time t. It is this quantity $(-)x_f$, which represents the

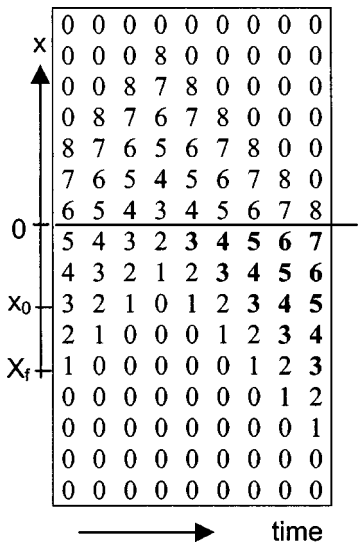

FIG. 3. Evolution of tracer exchange in a finite single-file system close to its boundary (lower part), represented by an infinite single-file system by assuming that molecules passing $x=0$ from above become tagged (indicated in bold). The numbers indicate the positions of eight adjacent particles in the (infinitely extended reference) system.

length of the section of the single-file system, which is occupied by tagged particles at time t. Hence, the tracer exchange curve results as

$$\gamma_{(\mathrm{ii})}(t)=\frac{2}{L}\int_{x_0=-\infty}^{0}\int_{x_f=-\infty}^{0}P(x_0,x_f,t)(-x_f)dx_f dx_0. \tag{3}$$

For further calculation, it is sufficient to preserve the assumption that the probability (density) $P(x,t)$ of particle displacement in the considered finite single-file system (the ''propagator'') is equal to that in the infinitely extended reference system for $x<0$. In doing so, we clearly do not make any assumptions about the evolution of the particle arrangement on ''the external'' side of the system $(x>0)$. The probability density that a particle starting at x_0 gets to x_f by time t, if at $x=0$ there is an absorbing boundary, is equal to (see Ref. [20])

$$P_{\mathrm{abs}}(x_0,x_f,t)=P(x_f-x_0,t)-P(-x_f-x_0,t), \tag{4}$$

where we have again benefited from the fact that the propagation probability in the infinite single-file system follows the pattern of normal diffusion (i.e., of a single-particle Markov process) if it is considered to evolve in $\sqrt{t}$ rather than in t. The probability (density) under the influence of an adsorbing wall may be correlated with the above introduced probability (density) $P(x_0,x_f,t)$ in the following way. Let us consider the probability $P(x_0,x_f,t)dx_f$ that the most distant point of the trajectory of a particle, which starts at x_0 and ends at x_f, is in the interval $0\cdots dx$. This probability has obviously to coincide with the increase in the probability finding a particle starting at x_0 and ending at x_f, if an adsorbing boundary is shifted from $x=0$ to $x=dx$. $P(x_0,x_f,t)$ is thus found to be the spatial derivative of $P_{\mathrm{abs}}(x_0,x_f,t)$. Since the shift by dx of the origin affects x_0 and x_f in the same way, with Eq. (4) the derivative of the first term on the right hand side vanishes, while the second term is doubled:

$$P(x_0,x_f,t)=2\frac{dP}{dx_0}(x=x_0+x_f,t)=2\frac{dP}{dx_f}(x=x_0+x_f,t). \tag{5}$$

Inserting Eq. (5) into Eq. (3) yields

$$\gamma_{(\mathrm{ii})}(t)=\frac{4}{L}\int_{x=-\infty}^{0}(-x)P(x,t)dx=\frac{1}{L}\sqrt{8/\pi\langle x^2(t)\rangle},$$

which is in fact identical with Eq. (2). Making use of the Gaussian shape of the propagator and the analytical expression [23,24]

$$\langle x^2(t)\rangle=2F\sqrt{t}=\frac{1-\theta}{\theta}\sqrt{2/\pi\tau}\sqrt{t} \tag{6}$$

for the mean square displacement in the case of single-file diffusion, we finally obtain

$$\gamma_{(\mathrm{ii})}=\frac{4}{L}\left(\frac{F\sqrt{t}}{\pi}\right)^{1/2}. \tag{7}$$

The time dependence $\gamma(t)\propto t^{1/4}$, as suggested by the respective parts of the simulation curves of tracer exchange, is thus confirmed by the analytical treatment. Since the above considered model ignores the existence of the time regime (i) Eqs. (6) and (7) cannot be expected to fully reproduce the proportionality factors between $\gamma(t)$ and $t^{1/4}$. The values of F from the best fit to the simulation data of Fig. 2 were by about one order of magnitude larger than those calculated using Eq. (6).

(iii) For further enhanced observation times, the molecular displacements are progressively stronger dominated by a diffusive movement of the whole file (the center-of-gravity diffusion) [8–10]. In the limit of fast exchange between the marginal sites and the surroundings, the corresponding diffusion coefficient has been determined to be [8,10]

$$D=\frac{(1-\theta)D_0}{L\theta}. \tag{8}$$

Tracer exchange under diffusion control is given by the relation [19]

$$\gamma_{\mathrm{diff}}(t)=1-\frac{8}{\pi^2}\sum_{n=0}^{n=\infty}\frac{1}{(2n+1)^2}\exp\left(\frac{-(2n+1)^2\pi^2Dt}{l^2L^2}\right), \tag{9}$$

and the product $\gamma(t)L$ ceases to be invariant with the file length.

Included in Fig. 1 are also the concentration profiles, obtained by assuming that (a) the tracer exchange in the inner part of length L^* is governed by diffusion, and (b) the marginal parts of the file are instantaneously filled with tagged

TABLE I. Relations between the results of the best fit $D_{(iii)}$ and L^* and the center-of-mass diffusivity D and file length L in the final time domain of tracer exchange (controlled by center-of-mass diffusion).

L	$D_{(iii)}/D$	L^*/L
150	1.51	0.83
300	1.49	0.87
600	1.8	0.92

particles. For all considered cases, in this way the conception of diffusion-controlled tracer exchange [19]

$$\frac{q(x,t)}{q_1} = 1 - \frac{4}{\pi}\sum_{n=0}^{n=\infty}\frac{(-1)^n}{2n+1}\left[\cos\frac{(2n+1)\pi(x-L^*/2)}{L^*}\right] \times \exp\left(\frac{-(2n+1)^2\pi^2 Dt}{L^{*2}}\right) \tag{10}$$

yielded a satisfactory analytical expression of the simulated profiles. Table I shows the relation between the diffusivities of the best fit ($D_{(iii)}$) and the values following from Eq. (8) as well as the relation between L^* and L. Taking into account that, in the considered time regime, molecular exchange in the marginal parts of the system (of total length $L-L^*$) already has been completed, the tracer exchange curve may be noted as

$$\gamma_{(iii)}(t) = \frac{L-L^*}{L} + \frac{L^*}{L}\gamma_{diff}(t), \tag{11}$$

with the values of L^* and $D_{(iii)}$ as given in Table I.

Though a detailed, quantitative explanation of the correlations between the analytical and fitting parameters reported in this paper is still lacking, the time scaling of tracer exchange in all time regimes of tracer exchange in finite single-file systems could be satisfactorily reproduced by analytical considerations. The validation of the different regimes for tracer exchange kinetics in real nature is one of the current challenges of the experimental research. To our knowledge, the only detailed experimental investigation of particle exchange in single-file systems has been carried out with laser-polarized ^{129}Xe NMR spectroscopy [18]. The observed exchange pattern complies with the time regime (ii) of single-file diffusion. Finding examples for the entity of patterns and their mutual transitions remains an attractive task of future experimental work.

ACKNOWLEDGMENTS

The financial support by the German Science Foundation (the graduate college ''Physikalische Chemie der Grenzflächen'' and the SFB 294 ''Moleküle in Wechselwirkung mit Grenzflächen''), by the Max-Buchner Foundation, and by ''Fonds der Chemischer Industrie'' is gratefully acknowledged. The authors thank A. Pines for his helpful comments.

[1] J. M. Bennett, J. P. Cohen, E. M. Flanigen, J. J. Pluth, and J. V. Smith, ACS Symp. Ser. **218**, 109 (1983).
[2] Ch. Baerlocher, W. M. Meier, and D. H. Olson, *Atlas of Zeolite Framework Types* (Elsevier, Amsterdam, 2001).
[3] J. Kärger, M. Petzold, H. Pfeifer, S. Ernst, and J. Weitkamp, J. Catal. **136**, 283 (1992).
[4] V. Gupta, S. S. Nivarthi, A. V. McCormick, and H. T. Davis, Chem. Phys. Lett. **247**, 596 (1995).
[5] K. Hahn, J. Kärger, and V. Kukla, Phys. Rev. Lett. **76**, 2762 (1997).
[6] V. Kukla, J. Kornatowski, D. Demuth, I. Girnus, H. Pfeifer, L. V. C. Rees, S. Schunk, K. K. Unger, and J. Kärger, Science **272**, 702 (1996).
[7] D. S. Sholl and K. A. Fichthorn, Phys. Rev. Lett. **79**, 3569 (1997).
[8] K. Hahn and J. Kärger, J. Phys. Chem. B **102**, 5766 (1998).
[9] C. Rödenbeck and J. Kärger, J. Chem. Phys. **110**, 3970 (1999).
[10] P. H. Nelson and S. M. Auerbach, J. Chem. Phys. **110**, 9235 (1999).
[11] P. H. Nelson and S. M. Auerbach, Chem. Eng. J. **74**, 43 (1999).
[12] Chr. Rödenbeck, J. Kärger, and K. Hahn, Phys. Rev. E **55**, 5697 (1997).
[13] Chr. Rödenbeck, J. Kärger, and K. Hahn, Phys. Rev. E **57**, 4382 (1998).
[14] C. Rödenbeck, J. Kärger, H. Schmidt, T. Rother, and M. Rödenbeck, Phys. Rev. E **60**, 2737 (1999).
[15] Z. Karpinski, S. N. Gandhi, and W. M. H. Sachtler, J. Catal. **141**, 337 (1993).
[16] G. D. Lei, B. T. Carvill, and W. M. H. Sachtler, Appl. Catal., A **142**, 347 (1996).
[17] F. J. M. M. de Gauw, J. van Grondelle, and R. A. van Santen, J. Catal. (to be published).
[18] T. Meersmann, J. W. Logan, R. Simonutti, S. Caldarelli, A. Comotti, P. Sozzani, L. G. Kaiser, and A. Pines, J. Phys. Chem. **104**, 11 665 (2000).
[19] J. Crank, *The Mathematics of Diffusion* (Claredon, Oxford, 1975).
[20] J. Kärger and D. M. Ruthven, *Diffusion in Zeolites and Other Microporous Solids* (Wiley, New York, 1992).
[21] N. Y. Chen, T. F. Degnan, and C. M. Smith, *Molecular Transport and Reaction in Zeolites* (VCH, New York, 1994).
[22] N. L. Filippova, Langmuir **13**, 5383 (1997).
[23] J. Kärger, Phys. Rev. A **45**, 4173 (1992).
[24] P. A. Fedders, Phys. Rev. B **17**, 40 (1978).